

# Mixing of post-discharge O<sub>2</sub>/He flow with NO<sub>2</sub>/He flow: 3D modeling of experimental data

T.V. Rakhimova<sup>a</sup>, A.P. Palov<sup>b</sup>, Yu.A. Mankelevich<sup>a</sup>, N.A. Popov<sup>a</sup>, and D.L. Carroll<sup>c</sup>

<sup>a</sup>Skobeltsyn Institute of Nuclear Physics, Moscow State University, 119992, Russia

<sup>b</sup>Plasma Venture Ltd, Moscow, Mosfilmovskaya 17b, 119330, Russia

<sup>c</sup>CU Aerospace, 2100 S. Oak St. – Suite 206, Champaign, IL 61820, USA

## ABSTRACT

Flow mixing and chemical kinetics in the afterglow of an electro-discharge source of singlet oxygen O<sub>2</sub>(a<sup>1</sup>Δ<sub>g</sub>) are studied theoretically using both a simple analytical approach and an advanced three-dimensional (3D) simulation with the FLUENT code. Calculated results are compared with titration measurements of atomic oxygen flow in the discharge oxygen-iodine laser (DOIL) system in which the first positive gain and continuous-wave laser oscillation were demonstrated [1,2]. It was shown [1] that atomic oxygen atoms in rf post-discharge O<sub>2</sub>/He mixtures effectively deplete O<sub>2</sub>(a<sup>1</sup>Δ<sub>g</sub>) molecules through quenching of the excited iodine atoms. Thus, the precise technique for O atom flow measurements and methods of removing O atoms are of importance for DOIL operation. One technique is through the admixing of NO<sub>2</sub> to the post-discharge flow which allows control of the O atom flow. Theoretical predictions of NO<sub>2</sub>\* production (and equivalently the emission), using both an analytical solution of a simplified system of equations and thorough 3D modeling of the reactive mixing flows, are compared with experimental measurements of NO<sub>2</sub>\* emission. Analysis of 3D calculated distributions of species concentrations and flow velocities shows how titration measurements should be calibrated correctly and validates the use of a simple analytical approach for the interpretation of titration measurements. It is recommended that NO<sub>2</sub> titrations for the flow conditions near to those examined use the value obtained from fully extinguishing the NO<sub>2</sub>\* emission.

**Keywords:** oxygen-iodine laser, titration, afterglow mixture, three-dimensional modeling

## 1. INTRODUCTION

The population inversion on iodine I(<sup>2</sup>P<sub>1/2</sub>) → I(<sup>2</sup>P<sub>3/2</sub>) electronic transition (1315 nm) in oxygen-iodine laser (OIL) systems is produced by the near resonant energy transfer from the metastable singlet oxygen molecule O<sub>2</sub>(a<sup>1</sup>Δ<sub>g</sub>). The development of effective pumping sources of O<sub>2</sub>(a<sup>1</sup>Δ<sub>g</sub>) based on a compact electric discharge system will reduce operational cost and laser system size and weight, increase operational safety and result in a wider application field of DOIL in comparison with classical chemical OIL (COIL). Substantial progress in DOIL development was achieved during the last three years. Continuous-wave laser power (now up to 1.5 W [3]) was demonstrated in DOIL system based on a capacitive rf discharge in flowing, low pressure O<sub>2</sub>/He mixture with an optimal O<sub>2</sub> partial pressure in the discharge region of about 3.7 Torr [3]. Enhancement of laser power should be obtainable at elevated oxygen pressures while preserving the same level of O<sub>2</sub>(a<sup>1</sup>Δ<sub>g</sub>) yields. However, O<sub>2</sub>(a<sup>1</sup>Δ<sub>g</sub>) yields come down with O<sub>2</sub> pressure in this longitudinal rf discharge system. On the other hand, recently record O<sub>2</sub>(a<sup>1</sup>Δ<sub>g</sub>) yields of 15-20% have been achieved in elevated pressure transverse rf discharge systems (P<sub>O<sub>2</sub></sub> ~ 10-20 Torr, rf frequency of 81 MHz) with heterogeneous removal of O atoms in the plasma and post-discharge regions using a HgO coating and cooling of the discharge tube wall [4]. It was shown in [5,6] that high atomic oxygen mole fractions result in depletion of O<sub>2</sub>(a<sup>1</sup>Δ<sub>g</sub>) yields via several quenching processes; one of these processes, namely, O<sub>2</sub>(a<sup>1</sup>Δ<sub>g</sub>) + O + M ⇒ O<sub>2</sub> + O + M becomes increasingly important with oxygen pressure. In addition to the direct quenching of O<sub>2</sub>(a<sup>1</sup>Δ<sub>g</sub>) molecules by O atoms in the plasma and post-discharge regions there is another effective mechanism of O<sub>2</sub>(a<sup>1</sup>Δ<sub>g</sub>) depletion involving O and iodine (I) atoms. In previous research [1] it was shown that even small mole fractions of O atoms (e.g. atoms that have survived after insufficient NO<sub>2</sub> addition) effectively deplete the O<sub>2</sub>(a<sup>1</sup>Δ<sub>g</sub>) through quenching of the excited iodine atoms, and this made lasing impossible until the

problem was understood. Thus, methods of controlling and removing O atoms from the afterglow region and the simulation of relevant processes of gas flow mixing and chemical kinetics are of importance for creating the electro-discharge oxygen-iodine laser. We have theoretically studied the post-discharge O<sub>2</sub>/He/NO<sub>2</sub> mixture dynamics for one set of experimental conditions where positive gain was attained [1]. Estimates of O atom flow rates are presented based on matching of the analytical model and/or 3D model calculations of NO<sub>2</sub>\* production with experimental measurements of NO<sub>2</sub>\* emission. Analysis of the 3D calculated distributions of species concentrations and flow velocities shows how titration measurements should be calibrated correctly and validates the use of a simple 1D analytical approach for determination of O atom flow rates.

## 2. EXPERIMENTAL SETUP

A block diagram of the typical flow tube setup for laser operation is shown in Fig. 1. Upstream of the supersonic nozzle, the subsonic diagnostic duct has four windows for optical emission and gain/absorption measurements. Optical emission data are also taken directly through glass tubes in the flow system, which can be reconfigured for a variety of studies. The broadband emission of NO<sub>2</sub>\* at ~25 cm downstream from the NO<sub>2</sub> ring was measured using a Hamamatsu R955 photomultiplier with a narrowband 580 nm filter and a 50 mm focal length Pyrex collection lens. All optical diagnostics were fiber coupled using Oriel model #77538 glass fiber bundles. For titration measurements, the NO<sub>2</sub> injection ring was located 53 cm downstream from the discharge exit, the O atom measurement position (NO<sub>2</sub>\* radiation detection) and the I<sub>2</sub>/He injection ring were located ~78 cm and 82 cm downstream from the discharge exit, respectively. Typical experimental conditions for which positive gain and lasing have been detected are following: gas pressure of 12.5 Torr, flow rates of 3 mmol/s and 16 mmol/s of O<sub>2</sub> and He, respectively, tube diameter of 4.9 cm, average flow velocity of ~18 m/s, 13.56 MHz rf discharge input powers of 400 - 770 W. Variable NO<sub>2</sub> flow with 2 mmol/s of He carrier gas was injected into the main stream through 8 small holes on the inside of the NO<sub>2</sub> injector ring.

The expected parabolic shape of the NO<sub>2</sub> flow rate dependence of NO<sub>2</sub>\* assumed in the standard titration measurement scheme [7] (which titrates to the peak of the NO<sub>2</sub>\* intensity emission, and multiplies that result by 2x to determine the O atom flow rate) resulted in the following conclusion for conditions similar to those above [1]: removal of almost all of O the atoms due to NO<sub>2</sub> admixing was attained with a significant excess of the NO<sub>2</sub> flow rate (e.g. an NO<sub>2</sub> flow rate of 1 mmol/s was required to fully remove the O atoms where the titration technique of observing the peak of the emission resulted in a measured O atom flow rate of 0.59 mmol/s). On the other hand, three-dimensional simulations (using the FLUENT code) of these experimental conditions (NO<sub>2</sub> injection, flow mixing, heat and mass transfer, chemical kinetics and diffusion) show that the NO<sub>2</sub> flow that is just equal to the local O atom flow is quite sufficient to dramatically reduce the O-atom flow downstream from the NO<sub>2</sub>/He injection ring. These observations suggest that standard titration procedure may significantly underestimate the measured O atom flow rates (by a factor of as much as 1.5 – 2.5) in post-discharge O<sub>2</sub>/O<sub>2</sub>(a<sup>1</sup>Δ<sub>g</sub>)/O/He mixtures and it is necessary to recalibrate the O atom titration measurement technique for such flow conditions. 3D model calculations and a 1D analytic approach described below shows how the adjustment should be performed.

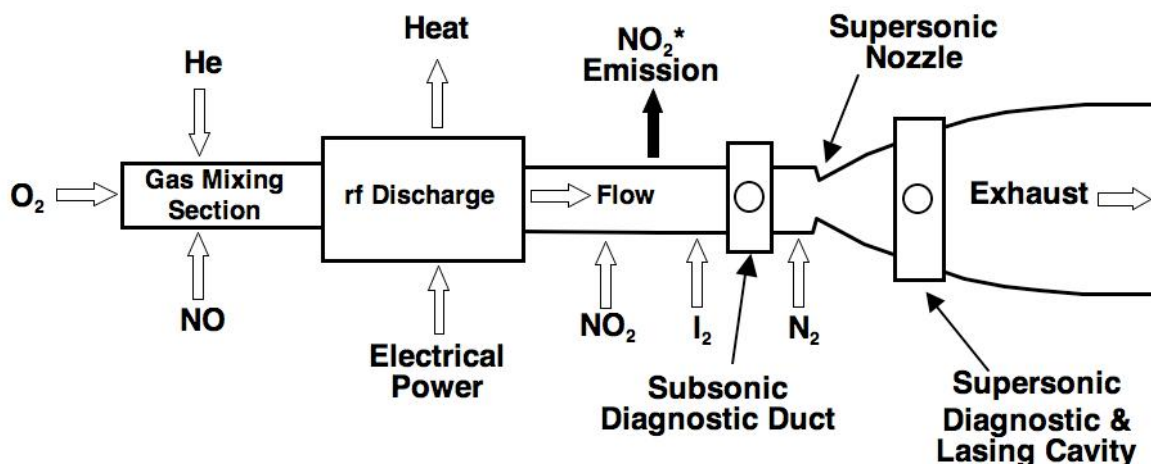
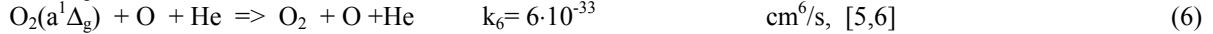
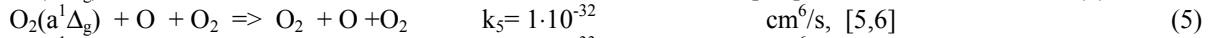
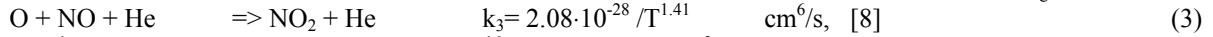
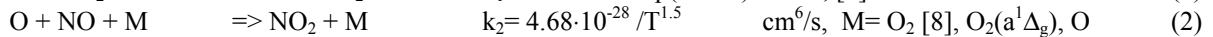
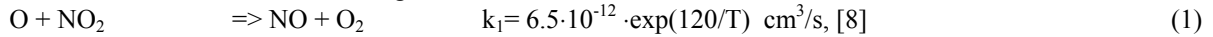


**Fig.1. Schematic of the ElectricOIL experimental apparatus.**

### 3. ANALYTICAL APPROACH AND 3D MODELING

The chemical kinetics and transport processes in post-discharge O/N/He flowing reactive mixtures were calculated with the FLUENT code in the subsonic region starting from an axial position just upstream from the NO<sub>2</sub>\* radiation measurements were made. Experimental flow rates for the O<sub>2</sub>/He discharge mixture and NO<sub>2</sub>/He admixture were taken as boundary conditions. The O atom flow in the post-discharge mixture was a variable parameter. The initial gas temperature was assumed to be 300 K. In 3D FLUENT calculations, conservation equations for mass, momentum, energy, and species concentrations, together with boundary conditions, thermal and caloric equations of state, are solved numerically in rectangular (xyz) coordinates on an adaptive grid with more than 100000 cells.

For prediction of NO<sub>2</sub>\* production rate we have used a simplified kinetic scheme that includes 6 species O, O<sub>2</sub>(a<sup>1</sup>Δ<sub>g</sub>), O<sub>2</sub>, He, NO, NO<sub>2</sub> and the following reaction mechanism:



Excited NO<sub>2</sub> states are also a transient product of reactions (2)-(3) and are stabilized by collisions with third bodies in vibrationally excited states and, in small part, by the radiative state of NO<sub>2</sub> whose decay produces the detected NO<sub>2</sub>\* emission. Thus, the calculated result of the combined theoretical-experimental titration scheme is a function I<sub>model</sub> proportional to the NO<sub>2</sub>\* radiation intensity

$$I_{\text{model}} = n_{\text{O}} \cdot n_{\text{NO}} \cdot kM \quad (7)$$

and integrated over the space volume which was measured as an experimentally detected intensity I<sub>measured</sub> of NO<sub>2</sub>\* , and kM is taken as kM = k<sub>2</sub>·(n<sub>O2</sub>+n<sub>O2(a)</sub>+n<sub>O</sub>)+k<sub>3</sub>·n<sub>He</sub> . Comparison of normalized data I<sub>measured</sub> (as a function of NO<sub>2</sub> flow rate) and calculated functions I<sub>model</sub> (as a function of the NO<sub>2</sub> and O atom flow rates) permitted the determination of the value of O atom flow rate which provides the best match to experimental data and thus determined the appropriate O atom mole fraction in the post-discharge regions. The results of the 3D FLUENT calculations permit a better understanding of the experiments.

A typical distribution of O atom mole fraction in the plane which intersects the tube axially through two opposing holes of the NO<sub>2</sub> injection ring is shown in Fig. 2 for base conditions: an initial discharge mixture of 3 mmol/s and 16 mmol/s of O<sub>2</sub> and He, respectively, a gas pressure of 12.5 Torr, and 0.2 mmol/s of NO<sub>2</sub> in 2 mmol/s of He flow through NO<sub>2</sub> injection ring. The O<sub>2</sub>(a<sup>1</sup>Δ<sub>g</sub>) flow rate in the post-discharge mixture were set equal to 0.6 mmol/s (20% yield), and the O atom flow rate was initially set to 0.6 mmol/s (but later varied to 0.45 and 0.25 mmol/s). The broad-band emission of NO<sub>2</sub>\* was collected from the tube cross-section as marked at 25 cm. Fig. 3 shows a magnified view of the O atom concentration in the same plane, and an example of the adaptive grid which typically consisted of ~120000 cells. Fig. 4 shows the flow velocity fields with typical parabolic profiles, and colors of the velocity arrows correspond to O<sub>2</sub>(a<sup>1</sup>Δ<sub>g</sub>) mole fractions. The distribution of NO mole fraction is shown in Fig. 5. Flow mixing effects are clearly seen in these figures. As is seen from Fig.3 and 5, NO is distributed almost uniformly over the tube cross-section at the NO<sub>2</sub>\* detection region in contrast with O atom concentration which peaks at the axis z, r=0. According to equation (7) this means that the main contribution to the NO<sub>2</sub>\* radiation intensity I<sub>measured</sub> and I<sub>model</sub> (see eq.(7)) is from the central core of the tube (r~0) and knowledge of the species concentrations only in this core can provide the reliable predictions of the NO<sub>2</sub>\* radiation intensity.

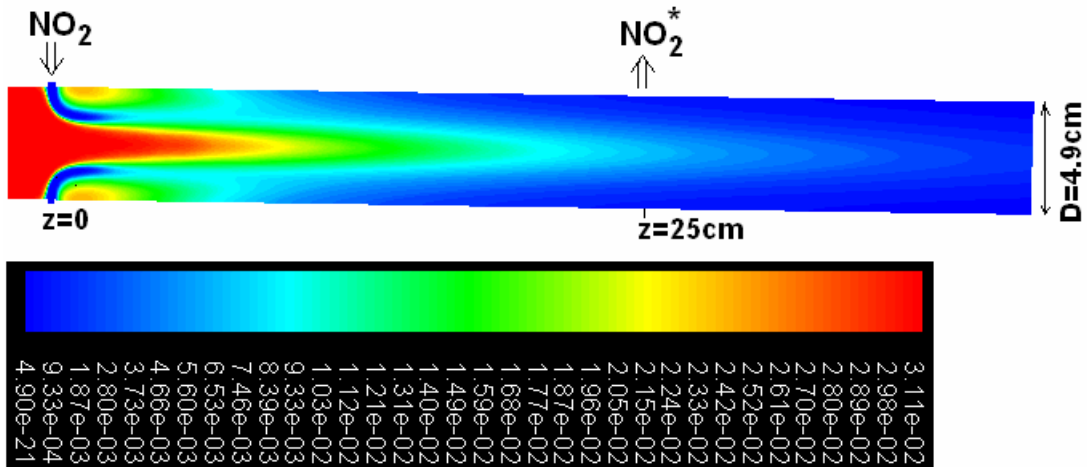


Fig.2. FLUENT calculated distributions of O atoms mole fraction. Flow rates through NO<sub>2</sub> injection ring: 0.2 mmol/s NO<sub>2</sub> / 2 mmol/s He. Post-discharge mixture flow rates: 0.6 mmol/s of O atoms, 0.6 mmol/s of O<sub>2</sub>(a<sup>1</sup>Δ<sub>g</sub>), 2.1 mmol/s of O<sub>2</sub> and 16 mmol/s of He.

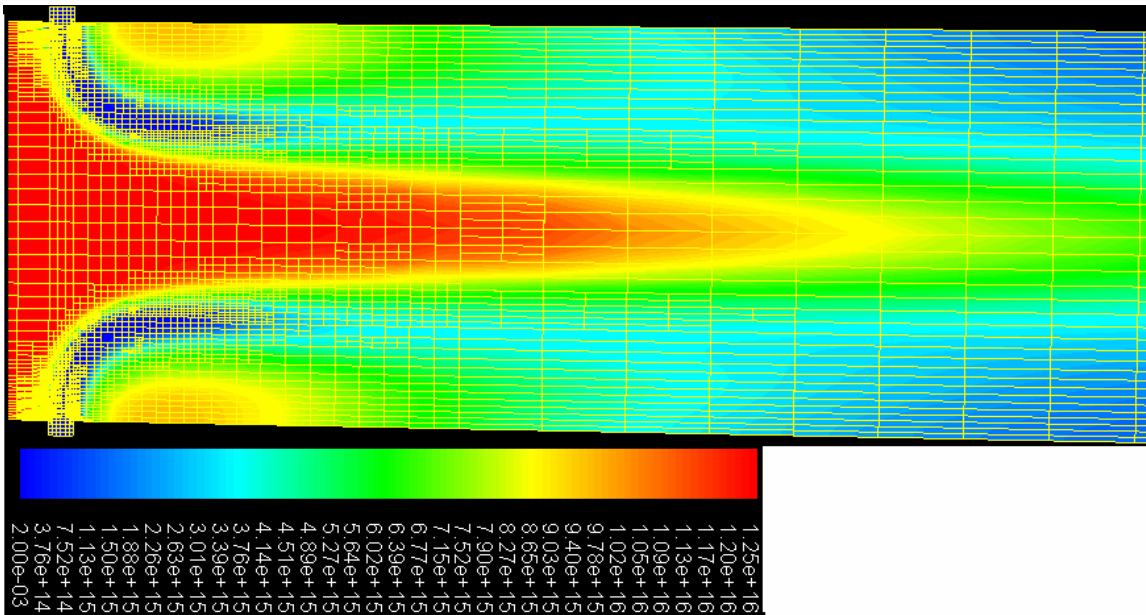


Fig.3. FLUENT calculated distributions of O atoms concentrations for the conditions of Fig.2 and used adaptive grid.

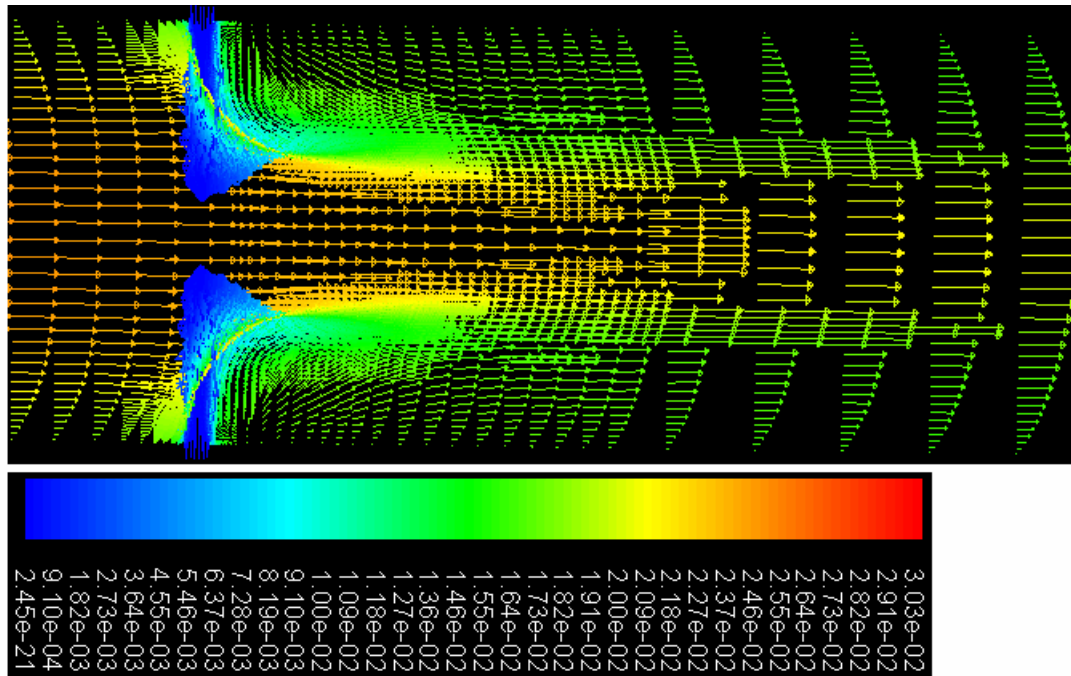


Fig.4. FLUENT calculated distributions of flow velocities for the conditions of Fig.2. Colors of the velocity arrows correspond to  $O_2(a^1\Delta_g)$  mole fractions.

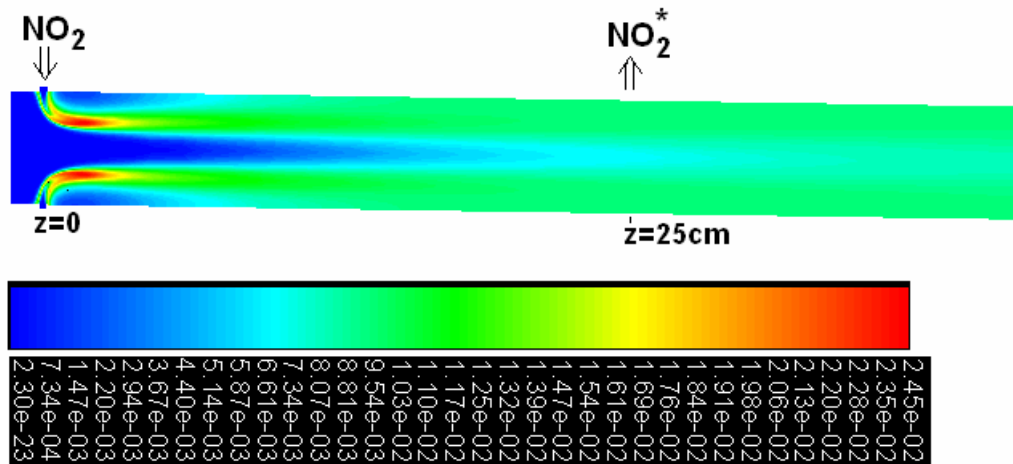


Fig.5. FLUENT calculated distributions of NO atoms mole fraction for the conditions of Fig.2.

Balance equations for O, NO and  $NO_2$  species concentration  $n_i$  at the axis  $z$  can be solved analytically if we assume constant velocity at the axis ( $r=0$ )  $v_0=2v_{\text{average}}$  ( $v_{\text{average}}=17.5$  m/s is an average flow velocity for the base conditions) and take into account the production and loss terms from reactions 1- 3:

$$dn_i / dt = S_i - L_i \cdot n_i, \quad t = [0, t_1] \quad (8)$$

Here  $i=O, NO, NO_2$  and transport time  $t_1 = (z_{NO_2^*} - z_{NO_2\text{ring}})/v_0$ . For the experimental conditions,  $k_1 \gg kM$  and equation system (8) can be analytically solved. As a result, we find  $n_O \cdot n_{NO}$  and thus  $I_{\text{model}}$  at the axial position  $z_{NO_2^*}$  of the  $NO_2^*$  radiation detector as a function of a given  $NO_2$  flow rate  $F_{NO_2}$  and initial O atom flow rate  $F_O$  at the  $NO_2$  injection ring:

$$n_O \cdot n_{NO} = NO_{2_{ini}} \cdot (O_{ini} - NO_{2_{ini}}) \cdot \exp(-2 \cdot NO_{2_{ini}} \cdot kM \cdot t1) \quad (9)$$

Here initial concentrations of  $NO_2$  and  $O$  are expressed as  $NO_{2_{ini}} = N \cdot F_{NO_2} / F$  and  $O_{ini} = N \cdot F_O / F$ ,  $N$  and  $F$  are the total gas concentration and total flow rate respectively. As is seen from Eq. (9), the classic parabolic dependence of the  $NO_2^*$  emission intensity will be observed only if  $2 \cdot NO_{2_{ini}} \cdot kM \cdot t1 \ll 1$ . However, this is not the case for the experimental flow conditions and  $I_{model}$  is really a more complex function with one maximum at

$$NO_{2_{ini}} = 0.5 \cdot O_{ini} + 1/(2 \cdot kM \cdot t1) - (0.25 \cdot O_{ini}^2 + 1/(2 \cdot kM \cdot t1)^2)^{0.5} \quad (10)$$

and  $I_{model}=0$  at  $F_{NO_2} = F_O$ . Curves of this analytic function (7) as well as 3D FLUENT calculated results, for different  $O$  atom flows  $F_O$ , and the experimental data [9]  $I_{measured}$  for the base conditions are shown in Fig. 6. All functions are normalized to unity. As is seen, the analytic functions are in reasonably good agreement with available 3D FLUENT results for  $F_O=0.25$  and  $0.45$  mmol/s (note that 3D calculations require a lot of computational time and only three cases were run with  $0.60$  mmol/s). The analytic function for  $F_O=0.54$  mmol/s provides the best approximation of the maximum intensity position ( $NO_2$  flow rate) and tail (at  $F_{NO_2} > 0.41$  mmol/s) of the experimental curve  $I_{measured}$ . It should be noted that the best correlations of analytic functions and experimental data should be observed in the tail region  $F_{NO_2} \sim F_O$  where only the central core flow volume ( $r \sim 0$ ) contributes to the measured  $NO_2^*$  radiation. Note that the experimental data show a higher intensity than do either the analytical model or the 3D simulations in the range  $0.20 < F_O < 0.40$ ; this may be due to the assumption in the models that the flow temperature was  $300$  K, when in reality the flow temperature was more likely around  $450$  K at the exit of the discharge and cooled with flow distance, combined with the fact that reaction rates (2) and (3) are slower with higher temperature. Regardless, the combined theoretical-experimental approach allows one to determine the atomic oxygen flows in post-discharge mixtures using the tail of the titration curves, e.g.  $F_O \sim 0.54$  mmol/s provides the best match for experimental titration data under consideration. 3D FLUENT calculations clearly show (Fig. 2 and 5) that incomplete flow mixing at short transport times  $t1$  affects the radial distribution of species concentrations and complicates the interpretation of titration measurements.

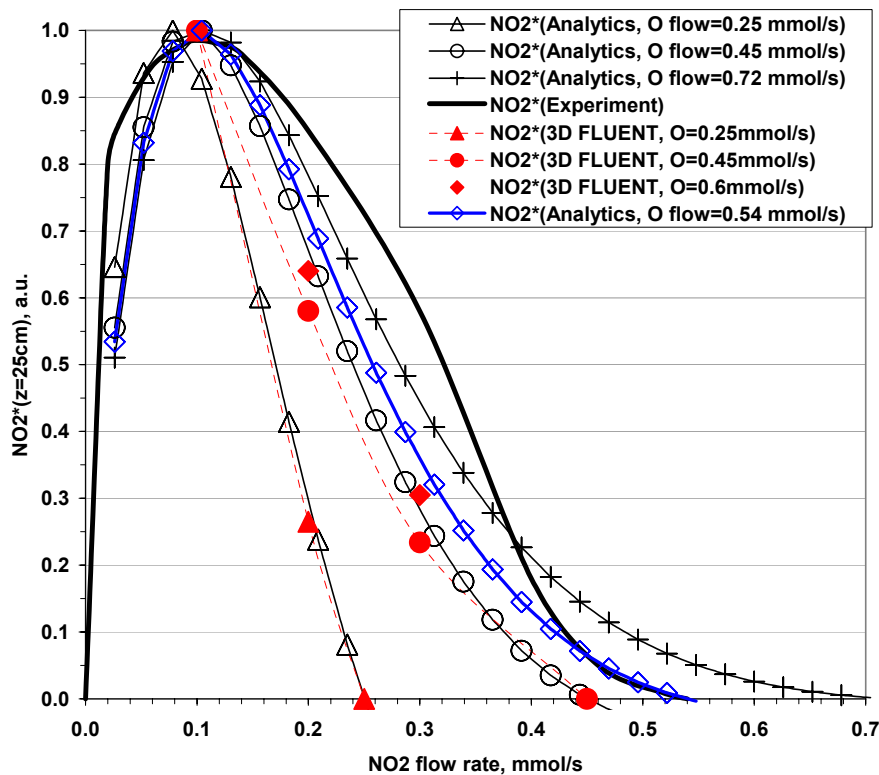


Fig.6. Normalized experimental and theoretical  $NO_2^*$  radiation intensities as functions of  $O_2$  flow rates. Analytics,  $T=300K$ ,  $t1 = 7.1$  ms,  $kM=2.83e-14$  cm<sup>3</sup>/s

Note that in [9] the reported O atom flow rates for these conditions were  $\sim 0.20$  mmol/s; an estimate based upon twice (2x) the NO<sub>2</sub> flow rate at the peak of the intensity profile. These results indicate that using the peak results in an underestimate of the O atom flow by a factor of  $\sim 2.5$  for these flow conditions, and that it would be more accurate to use a titration to the point where the NO<sub>2</sub>\* emission is extinguished (at the tail end of the titration). It should be pointed out that the standard NO<sub>2</sub> titration is still valid for slow flow, low pressure conditions such as those in [7].

#### 4. CONCLUSIONS

We have theoretically studied the post-discharge O<sub>2</sub>/He mixture dynamics of experimental conditions where the first positive gain and continuous-wave laser oscillation in the ElectricOIL laser were attained [1,2]. In previous research it was shown [1] that even small mole fractions of O atoms (e.g. atoms that have survived after insufficient NO<sub>2</sub> addition) effectively deplete the O<sub>2</sub>(a<sup>1</sup>Δ<sub>g</sub>), and this made lasing impossible until the problem was understood. Thus, methods of removing O atoms from the afterglow region and the simulation of relevant processes of gas flow mixing and chemical kinetics are of importance for enhancing the electro-discharge oxygen-iodine laser. Three-dimensional simulations (using the FLUENT code) of rf post-discharge processes (NO<sub>2</sub> injection, flow mixing, heat and mass transfer, chemical kinetics) show that the NO<sub>2</sub> flow that is just equal to the local O atom flow is quite sufficient to dramatically reduce the O-atom flow downstream from the NO<sub>2</sub>/He injection ring. Calculations show that the expected parabolic shape of the NO<sub>2</sub> flow rate dependence of NO<sub>2</sub>\* emission assumed in the standard titration measurement scheme is seriously affected in these fast flow, higher pressure experimental conditions. Post-discharge NO<sub>2</sub> admixing permits the control of O atoms flow and analysis of 3D calculated distributions of species concentrations and flow velocities shows how titration measurements should be calibrated correctly. The 3D modeling also validates the use of the developed analytical approach for interpreting the titration measurements. A calibration procedure based on comparison and matching of calculated NO<sub>2</sub>\* production rate and measured NO<sub>2</sub>\* radiation as functions of NO<sub>2</sub> flow rates potentially allows a more accurate determination of the O atom flow rates, and shows that titration to tail of the NO<sub>2</sub>\* emission provides a more accurate measurement of the O atom flow rate.

#### ACKNOWLEDGEMENTS

The work is partially funded from the CRDF project RUP1-5044-MO-05, RFBR project 06-02-16537 and RF Presidential Program SS-7101.2006.2.

#### REFERENCES

1. D.L. Carroll, J.T. Verdeyen, D.M. King, J.W. Zimmerman, J.K. Laystrom, B.S. Woodard, G.F. Benavides, K. Kittell, and W.C. Solomon, *IEEE J. Quant. Elect.* **41**(2), 213-223 (2005).
2. D. L. Carroll, J. T. Verdeyen, D. M. King, J. W. Zimmerman, J. K. Laystrom, B. S. Woodard, G. F. Benavides, K. Kittell, D. S. Stafford, M. J. Kushner, and W. C. Solomon, *Appl. Phys. Lett.*, **86**, 111 104-1-3 (2005).
3. D. M. King, D. L. Carroll, J. T. Verdeyen, J. K. Laystrom, G. F. Benavides, A.D. Palla, J. W. Zimmerman, B. S. Woodard, and W. C. Solomon, "Power Enhancement of the Hybrid ElectricOIL System," AIAA Paper 2006-3756.
4. T. V. Rakhimova, A. S. Kovalev, K. S. Klopovsky, D. V. Lopaev, Yu. A. Mankelevich, A. N. Vasilieva, O. V. Braginsky, N. A. Popov, O. V. Proshina, and A. T. Rakhimov, "Singlet oxygen generator operating at high oxygen pressure" *AIAA 37th Plasmadynamics and Lasers Conf.*, San Francisco, Paper no. 2006-3762 (2006). See also T. V. Rakhimova, O. V. Proshina et al, "Pressure scaling of an ED SOG" at GCL/HPL", Gmunden, Austria (2006).
5. O.V. Braginskiy, A.N. Vasilieva, K.S. Klopovskiy, A.S. Kovalev, D.V. Lopaev, O.V. Proshina, T.V. Rakhimova and A.T. Rakhimov, *J. Phys. D: Appl. Phys.* **38**, 3609-3625 (2005)
6. O.V. Braginskiy, A.N. Vasilieva, A.S. Kovalev, D.V. Lopaev, Yu.A. Mankelevich, T.V. Rakhimova and A.T. Rakhimov, *J. Phys. D: Appl. Phys.* **38**, 3626-3634 (2005)
7. F. Kaufman, "The air afterglow and its use in the study of some reactions of atomic oxygen," *Proc. Roy. Soc. A*, **247**, 123-139 (1958).
8. R. Atkinson, D. L. Baulch, R. A. Cox, R. F. Hampson Jr., J. A. Kerr, M. J. Rossi, and J. Troe, *J. of Phys and Chem. Ref. Data*, v. 26, 550-962 (1997).
9. J.W. Zimmerman, D.M. King, A.D. Palla, J.T. Verdeyen, D.L. Carroll, J.K. Laystrom, G.F. Benavides, B.S. Woodard, W.C. Solomon, W.T. Rawlins, S.J. Davis, and M.C. Heaven, "Important kinetic effects in the hybrid ElectricOIL system," Proc. of High Power Laser Ablation VI, ed. C.R. Phipps, SPIE **6261**, 62611R (2006).